PHYSICAL REVIEW B **81**, 104515 (2010)

Relaxation of nuclear magnetic moments and site-selective NMR in *d*-wave superconductors

Robert E. Throckmorton and Oskar Vafek

National High Magnetic Field Laboratory and Department of Physics, Florida State University, Tallahassee, Florida 32306, USA

(Received 7 September 2009; revised manuscript received 10 February 2010; published 15 March 2010)

A mechanism for relaxing the nuclear magnetic moments, in which a pair of spin-polarized BCS quasiparticles is emitted or absorbed, and which dominates at low temperature, is identified in type-II *d*-wave superconductors in an external magnetic field above H_{c1}. The results of the theory are compared with the NMR experiments on YBCO in high magnetic fields and found to agree without invoking antiferromagnetic order in the vortex core.

DOI: 10.1103/PhysRevB.81.104515 PACS number(s): 74.25.N−, 74.25.Ha, 74.72.−h

I. INTRODUCTION

Being a bulk real-space probe, with information about the precession and relaxation rates of nuclear spins at different sites inside the sample, NMR has served as one of the key experimental tools[1] in the study of the electronic properties of high-temperature cuprate superconductors (HTS). By and large, the ^{17}O NMR data[2–5] on HTS, in moderate to large magnetic fields, has been interpreted as evidence for antiferromagnetic (AF) order in the vortex core.[5–7] This interpretation was based on the dependence of the spin-lattice relaxation rate, $1/T_1$, for the Cu nuclei in the normal state; the rate remains constant with temperature,[8] as opposed to being linear in T, as predicted by the Korringa law.[9]

We reexamine this interpretation using analytical and numerical solutions of the Bogoliubov-de Gennes equations and find that the present data can be understood quantitatively without invoking AF ordering. In particular, the low-temperature upturn in $1/(T_1T)$ near the vortex core, but not away from it, can be understood to be caused by a combination of two effects: (1) the increase of the quasiparticle (qp) wave function near the core and (2) the shift of the minimum of the qp band with spin along the applied magnetic field (spin up) to negative energies due to Zeeman coupling. As a result, a new electronic channel opens up for relaxing the nuclear spin whereby a *pair* of spin-up quasiparticles is emitted or absorbed. This is in contrast to the standard "spin-flip" channel, in which a spin-up(down) qp is destroyed and a spin down(up) qp is created. At temperatures below the Zeeman scale the latter channel freezes out since the number of qp's with spin anti-aligned with the B-field becomes thermally activated, and the former channel dominates. In addition, we find that the broad NMR line shape appears even in the extreme type-II limit, where the diamagnetic response of the H-field induced supercurrents can be neglected. The broadening here is found to be due to the spatially nonuniform *paramagnetic* response of *d*-wave superconductors in the vortex state.

Several other theoretical investigations of NMR in the mixed state of the cuprate superconductors have been carried out. One of the earliest treatments was that of Takigawa *et al.*[10] using a self-consistent method of solution of the Bogoliubov-de Gennes equations due to Wang and MacDonald.[11] They found that $1/T_1$ is linear in temperature near the vortex cores at low temperatures and exhibits a small Hebel-Slichter-like peak near the superconducting transition temperature. At low temperature, the rates near the core are also found to be larger than the rates away from it, which approach the usual T^3 dependence. NMR in the *d*-wave mixed state was also studied using a semiclassical approach,[12] and using a linearized form of the Bogoliubov-de Gennes equations.[13] The results of the linearized model give faster rates near the vortex cores than away from them. They found that $1/(T_1T)$ near the core increases slowly with temperature up to 30 K, and remains almost constant over the same temperature range away from the core. Importantly, these works focused on the quasiparticle spin-flip channel, but, as mentioned above and as we show in more detail below, the Zeeman coupling of the quasiparticles, which cannot be ignored at large magnetic fields, introduces an additional channel for spin-lattice relaxation which is found to dominate at low temperature.

Our paper is organized as follows. In Sec. II, we state the full Hamiltonian of our system and review the basic formulas for the Knight shift and $1/T_1T$. In Sec. III, we introduce our model for the electronic contribution to the Hamiltonian, derive the formulas for the Knight shift and $1/T_1T$ for this model, and present the results of our calculations. In Sec. IV, we discuss the possible influence of antiferromagnetic correlations. Finally, we present our conclusions in Sec. V.

II. KNIGHT SHIFT AND SPIN-LATTICE RELAXATION RATE

A. Basic Model

We will start by stating the Hamiltonian describing our system.

$$\hat{H} = \hat{H}_e + \hat{H}_n + \hat{H}_{hf}, \tag{1}$$

where $\hat{H}_e$ is the Hamiltonian of the electrons on their own, $\hat{H}_n$ is that of the nuclei on their own, and $\hat{H}_{hf}$ is the hyperfine interaction between the electrons and nuclei. The nuclear contribution is just the total energy of the nuclear spins in an applied magnetic field,

$$\hat{H}_n = -\gamma_n \hbar \sum_{\mathbf{r}} \hat{\mathbf{I}}(\mathbf{r}) \cdot \mathbf{B}, \tag{2}$$

where γ_n is the gyromagnetic ratio of the nuclei and $\hat{\mathbf{I}}(\mathbf{r})$ is the spin of the nucleus at $\mathbf{r}$. There are other terms present, such as quadrupole terms and interactions among the nuclei.[1,9,14] However, in large magnetic fields, which we will be considering here, these terms are small compared to the above magnetic term. The quadrupole terms lead to uneven splitting of the nuclear energies, and the interactions may lead to a slight broadening of the resonances of the nuclei.[9,14] We use the model of Shastry, Mila, and Rice[15,16] for the hyperfine interaction,

$$\hat{H}_{hf} = -\gamma_e \gamma_n \hbar^2 \sum_{\mathbf{r}\mathbf{r}'} A(\mathbf{r}-\mathbf{r}') \hat{\mathbf{I}}(\mathbf{r}) \cdot \hat{\mathbf{S}}(\mathbf{r}'), \tag{3}$$

where γ_e and γ_n are the gyromagnetic ratios of an electron and a nucleus, respectively, $\hat{\mathbf{I}}$ and $\hat{\mathbf{S}}$ are their respective spin angular momenta, and the coefficients $A(\mathbf{r})$ are the form factors for the hyperfine interaction.[15,16] Note that we are taking γ_e to have a negative value. The electronic contribution will be the subject of the next section.

To compare our results to experiments,[5,14] we will be interested in the relaxation rates and the Knight shifts for the in-plane ^{17}O atoms in YBCO. For these atoms, we include the contributions to the form factor $A(\mathbf{r})$ from both nearest- (n.n.) and next-nearest-neighbor (n.n.n.) copper atoms: $\gamma_e \gamma_n \hbar^2 A(\mathbf{r}-\mathbf{r}')$ is equal to 2.317×10^{-7} eV for the n.n. Cu atoms, and 5.794×10^{-8} eV for the n.n.n. Cu atoms.[17,18] As discussed by Zha, Barzykin, and Pines,[18] this form factor suppresses contributions from the AF correlations to the spin-lattice relaxation rate at O sites in the normal state. We expect this suppression to persist in the mixed state, as we will argue in Sec. IV.

B. Knight Shift

The Knight shift is a change (usually an increase) in the nuclear resonance frequency induced by the surrounding electrons.[9] This can be attributed to an effective magnetic field produced by the electrons through the hyperfine coupling to the nucleus. Using first-order time-independent perturbation theory on this term and taking the thermal average of the result, we get

$$\hat{H}_{hf,eff} = -\gamma_n \hbar \sum_{\mathbf{r}} \hat{\mathbf{I}}(\mathbf{r}) \cdot \delta \mathbf{B}_{eff}(\mathbf{r}), \tag{4}$$

where

$$\delta \mathbf{B}_{eff}(\mathbf{r}) = \gamma_e \hbar \sum_{\mathbf{r}'} A(\mathbf{r}-\mathbf{r}') \langle \hat{\mathbf{S}}(\mathbf{r}') \rangle \tag{5}$$

is the effective magnetic field experienced by the nuclei and produced by the electrons; $\langle . \rangle$ denotes a thermal average. Because the nuclear resonance frequency, $\omega = \gamma_n B$, is proportional to the applied magnetic field, this means that the resonance frequency is shifted by an amount $\gamma_n \delta B_{eff}$.

We will use this formula in the next section to determine the Knight shift in a d-wave superconductor in a magnetic field. Note that the above formulas, in general, allow for a position dependence of the effective magnetic field; the Knight shift in our system will, in fact, be position dependent.

C. Spin-Lattice Relaxation Rate

As is well known,[9] the spin-lattice relaxation rate at $\mathbf{r}$ is given by

$$\frac{1}{T_1(\mathbf{r})} = \frac{1}{2} \frac{\sum_{mn} W_{mn}(\mathbf{r}) (E_m - E_n)^2}{\sum_n E_n^2}, \tag{6}$$

where E_n is the energy of the nucleus at $\mathbf{r}$ in a state n, and it is assumed that $\Sigma_n E_n = 0$. We will also assume that the energies are equally spaced, i.e., $E_n - E_{n-1} = \delta E$. This is not exactly true, due to, for example, the quadrupole term, but, because we are working in high magnetic fields, such contributions beyond the magnetic energy are small, and we may treat the eigenstates of this term alone as almost exact, which is one of the assumptions made in the use of this formula.[9]

The function $W_{mn}(\mathbf{r})$ entering Eq. (6) is the transition rate for the z component (along the H-field) of the nuclear spin at site $\mathbf{r}$ to go from $m\hbar$ to $n\hbar$. We can find these rates using Fermi's Golden Rule,

$$W_{mn}(\mathbf{r}) = \frac{2\pi}{\hbar} \left\langle \sum_{QQ'} |\langle mQ'|\hat{V}(\mathbf{r})|nQ\rangle|^2 \delta(E_{mQ'} - E_{nQ}) \right\rangle, \tag{7}$$

where $V(\mathbf{r})$ is the hyperfine interaction in the form,

$$V(\mathbf{r}) = -\gamma_e \gamma_n \hbar^2 \sum_{\mathbf{r}'} A(\mathbf{r}-\mathbf{r}') \hat{\mathbf{I}}(\mathbf{r}) \cdot \hat{\mathbf{S}}(\mathbf{r}'). \tag{8}$$

We will employ these formulas to determine the spin-lattice relaxation rate in a d-wave superconductor in a magnetic field in the next section. Again, note that our formulas, in general, allow for a position dependence of the relaxation rate and the Knight shift.

III. NMR IN A d-WAVE SUPERCONDUCTOR

A. Bogoliubov-de Gennes (BdG) Equation

We now discuss the electronic contribution to the Hamiltonian. Our starting point will be the Hamiltonian for electrons on a square tight-binding lattice in a magnetic field with a singlet pairing term

$$\hat{H} = \sum_{\langle \mathbf{r}\mathbf{r}' \rangle} [t_{\mathbf{r}\mathbf{r}'} \hat{c}^\dagger_{\mathbf{r}\sigma} \hat{c}_{\mathbf{r}'\sigma} + \Delta_{\mathbf{r}\mathbf{r}'} (\hat{c}^\dagger_{\mathbf{r}\uparrow} \hat{c}^\dagger_{\mathbf{r}'\downarrow} - \hat{c}^\dagger_{\mathbf{r}\downarrow} \hat{c}^\dagger_{\mathbf{r}'\uparrow}) + \text{h.c.}] - \sum_{\mathbf{r}} \hat{c}^\dagger_{\mathbf{r}\alpha} (\mu \delta_{\alpha\beta} + h \sigma^z_{\alpha\beta}) \hat{c}_{\mathbf{r}\beta} \tag{9}$$

where the tight-binding hopping constants $t_{\mathbf{r}\mathbf{r}'}$ are $t_{\mathbf{r}\mathbf{r}'} = -te^{-i\mathcal{A}_{\mathbf{r}\mathbf{r}'}}$, $\mathcal{A}_{\mathbf{r}\mathbf{r}'} = \frac{e}{\hbar c} \int_{\mathbf{r}}^{\mathbf{r}'} \mathbf{A}(\mathbf{r}) \cdot d\mathbf{r}$; $\mathbf{A}(\mathbf{r})$ is the vector potential associated with the (constant) applied magnetic field $\mathbf{B}$, $\frac{1}{2} g \mu_B$ is the spin magnetic moment of an electron, and μ is

the chemical potential. For the symmetric gauge $\mathbf{A}(\mathbf{r})=\frac{1}{2}\mathbf{B}\times\mathbf{r}$, the values of $\mathcal{A}_{\mathbf{r}\mathbf{r}'}$ relevant for a square lattice are $\mathcal{A}_{\mathbf{r},\mathbf{r}+\hat{\mathbf{x}}}=-\pi y\Phi/\Phi_0$ and $\mathcal{A}_{\mathbf{r},\mathbf{r}+\hat{\mathbf{y}}}=\pi x\Phi/\Phi_0$, where Φ is the magnetic flux through a plaquette, and $\Phi_0=hc/e$ is the flux quantum. The pairing field $\Delta_{\mathbf{r}\mathbf{r}'}$ is assumed to have a constant magnitude and $\Delta_{\mathbf{r}\mathbf{r}'}=\eta_{\boldsymbol{\delta}}\Delta_0 e^{i\theta_{\mathbf{r}\mathbf{r}'}}$, where $\eta_{\pm\hat{\mathbf{x}}}=-\eta_{\pm\hat{\mathbf{y}}}=1$, otherwise $\eta_{\boldsymbol{\delta}}=0$. The phase factor $e^{i\theta_{\mathbf{r}\mathbf{r}'}}=[e^{i\phi(\mathbf{r})}+e^{i\phi(\mathbf{r}')}]/|e^{i\phi(\mathbf{r})}+e^{i\phi(\mathbf{r}')}|$, where $\phi(\mathbf{r})$ satisfies the equations, $\nabla\times\nabla\phi=2\pi\hat{\mathbf{z}}\Sigma_i\delta(\mathbf{r}-\mathbf{r}_i)$, where the $\mathbf{r}_i$ are the positions of the vortex cores, and $\nabla^2\phi=0$. These conditions determine $\phi(\mathbf{r})$ up to terms of the form $\phi_0+\mathbf{v}_0\cdot\mathbf{r}$; these constants are fixed by requiring zero overall current. The vortex cores form a periodic Abrikosov lattice, such that each primitive cell (magnetic unit cell) of this lattice carries exactly one quantum of magnetic flux hc/e. Note that our assumption of a constant magnetic field effectively corresponds to an infinite penetration depth. We choose to assume a pairing field of constant amplitude, placing all of the vortex physics into the phase. We do so because we believe that assuming a constant amplitude, as opposed to calculating it self-consistently, will not greatly affect our results. Lacking a microscopic model for cuprate superconductors, it is uncertain whether a self-consistent calculation will result in much improvement of our results. Finally, for notational convenience we denote the Zeeman factor by $h=\frac{1}{2}g\mu_B B$.

Our method of solution for this problem follows Refs. 19–21. To diagonalize this Hamiltonian, we introduce the singular gauge-Bogoliubov-de Gennes transformation[20,22]

$$\begin{bmatrix}\hat{c}_\uparrow(\mathbf{r})\\ \hat{c}_\downarrow^\dagger(\mathbf{r})\end{bmatrix}=\sum_{\mathbf{k}n}\begin{bmatrix}e^{i\phi(\mathbf{r})/2}u_{\mathbf{k}n}(\mathbf{r}) & -e^{i\phi(\mathbf{r})/2}v_{\mathbf{k}n}^*(\mathbf{r})\\ e^{i\phi(\mathbf{r})/2}v_{\mathbf{k}n}(\mathbf{r}) & e^{i\phi(\mathbf{r})/2}u_{\mathbf{k}n}^*(\mathbf{r})\end{bmatrix}\begin{bmatrix}\hat{\gamma}_{\mathbf{k}n\uparrow}\\ \hat{\gamma}_{\mathbf{k}n\downarrow}^\dagger\end{bmatrix},\tag{10}$$

which allows us to rewrite the Hamiltonian in terms of the quasiparticles in the Bloch basis corresponding to the magnetic unit cell $\ell_x\times\ell_y$ containing a pair of vortices. By Bloch's theorem the Nambu spinors, which are eigenfunctions of the Bogoliubov-de Gennes equation,[19,20,22] can be written as $[u_{\mathbf{k}n}(\mathbf{r}),v_{\mathbf{k}n}(\mathbf{r})]^T=e^{i\mathbf{k}\cdot\mathbf{r}}[U_{\mathbf{k}n}(\mathbf{r}),V_{\mathbf{k}n}(\mathbf{r})]^T$, where $U_{\mathbf{k}n}(\mathbf{r})$ and $V_{\mathbf{k}n}(\mathbf{r})$ are periodic in $\ell_x\times\ell_y$, n is the band index and the crystal momentum $\mathbf{k}\in(-\frac{\pi}{\ell_x},\frac{\pi}{\ell_x}]\times(-\frac{\pi}{\ell_y},\frac{\pi}{\ell_y}]$.

There is one issue introduced by this transformation that is worth addressing in detail. As we wind around a vortex, $\phi(\mathbf{r})$ increases by 2π. This means that the phase factors in the above gauge transformation only increase by π, meaning that the phase factors, at this point, are not uniquely determined. We must therefore introduce branch cuts into the Hamiltonian and choose the values of the phase factors carefully. The procedure we use in choosing the values of these factors is that used in Ref. 20. We first choose a branch cut, which can be any continuous curve connecting the two vortices inside the magnetic unit cell. We then choose one point $\mathbf{r}_0$ on the atomic lattice, and let the phase factor for that site be $b_0=e^{i\phi(\mathbf{r}_0)/2}$. We now move to a neighboring site $\mathbf{r}$ such that we do not need to cross the branch cut to reach it. Let b be the phase factor for this site. The solution to $b^2=e^{i\phi(\mathbf{r})}$ that we choose is the one that gives the lower value of $|b-b_0|$. We do this for all sites, thus generating the appropriate values for $e^{i\phi(\mathbf{r})/2}$. This process is illustrated in Fig. 1.

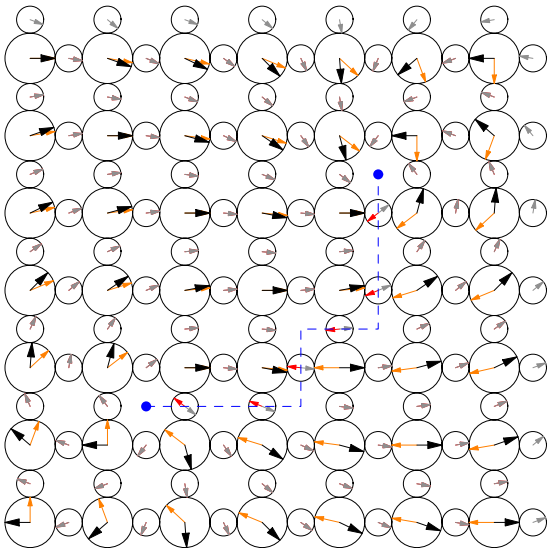

FIG. 1. (Color online) Illustration of the process by which we choose the values of $e^{i\phi(\mathbf{r})/2}$ for each site for a 6×6 magnetic unit cell. The large circles represent the sites, and the small circles the bonds connecting them. The dots are the locations of the vortex cores, and the dashed line is the branch cut. The black arrows represent the site phase factors, $e^{i\phi(\mathbf{r})}$, while the large gray (orange) arrows represent the value of $e^{i\phi(\mathbf{r})/2}$ chosen by the process outlined in the text. The bond phase variable, $e^{i\theta_{\mathbf{r}\mathbf{r}'}}$, is represented by the small light gray arrow, and $e^{i\phi(\mathbf{r})/2}e^{i\phi(\mathbf{r}')/2}$ is represented by the small dark gray (red) arrow.

The coefficients $U_{\mathbf{k}n}(\mathbf{r})$ and $V_{\mathbf{k}n}(\mathbf{r})$ satisfy the Bogoliubov-de Gennes equation, $e^{-i\mathbf{k}\cdot\mathbf{r}}\hat{\mathcal{H}}_0 e^{i\mathbf{k}\cdot\mathbf{r}}\Phi_{\mathbf{k}n}(\mathbf{r})=E_{\mathbf{k}n}\Phi_{\mathbf{k}n}(\mathbf{r})$, where $\Phi_{\mathbf{k}n}(\mathbf{r})=[U_{\mathbf{k}n}(\mathbf{r}),V_{\mathbf{k}n}(\mathbf{r})]^T$, $\hat{\mathcal{H}}_0=\sigma_z(\hat{\mathcal{E}}_{\mathbf{r}}-\mu)+\sigma_x\hat{\Delta}_{\mathbf{r}}-h$, the operators $\hat{\mathcal{E}}_{\mathbf{r}}$ and $\hat{\Delta}_{\mathbf{r}}$ are

$$\hat{\mathcal{E}}_{\mathbf{r}}=-t\sum_{\boldsymbol{\delta}=\pm\hat{\mathbf{x}},\pm\hat{\mathbf{y}}}z_{2,\mathbf{r},\mathbf{r}+\boldsymbol{\delta}}e^{i\sigma_z V_{\mathbf{r},\mathbf{r}+\boldsymbol{\delta}}}\hat{T}_{\boldsymbol{\delta}},$$

$$\hat{\Delta}_{\mathbf{r}}=\Delta_0\sum_{\boldsymbol{\delta}=\pm\hat{\mathbf{x}},\pm\hat{\mathbf{y}}}z_{2,\mathbf{r},\mathbf{r}+\boldsymbol{\delta}}\eta_{\boldsymbol{\delta}}\hat{T}_{\boldsymbol{\delta}},$$

and $\hat{T}_{\boldsymbol{\delta}}$ performs a translation along the vector $\boldsymbol{\delta}$.

We now wish to make a comment on the energies of the quasiparticles in our system. Let $\hat{\mathcal{H}}_{0,NZ}=\sigma_z(\hat{\mathcal{E}}_{\mathbf{r}}-\mu)+\sigma_x\hat{\Delta}_{\mathbf{r}}$—that is, $\hat{\mathcal{H}}_{0,NZ}$ is $\hat{\mathcal{H}}_0$ without the Zeeman term. Note that diagonalizing $\hat{\mathcal{H}}_{0,NZ}$ is the same as diagonalizing $\hat{\mathcal{H}}_0$ because the two differ only by a term proportional to the identity matrix. In fact, if we let $E_{\mathbf{k}n}$ be the eigenvalues of $\hat{\mathcal{H}}_{0,NZ}$, then the eigenvalues of $\hat{\mathcal{H}}_0$ are just $E=E_{\mathbf{k}n}-h$. The matrix $\hat{\mathcal{H}}_{0,NZ}$, as we implied, would replace $\hat{\mathcal{H}}_0$ if we neglected the Zeeman splitting. Since we can simultaneously diagonalize $\hat{\mathcal{H}}_0$ and $\hat{\mathcal{H}}_{0,NZ}$, we see that the same eigenvectors would diagonalize the difference between the two Hamiltonians that result in these matrices, which is a term proportional to the z component of the spin. This is because the z component of the spin is a good quantum number, and can be

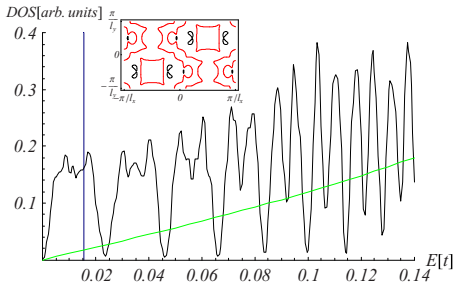

FIG. 2. (Color online) Density of qp states for $B=0$ (gray line; green online) and $B\approx 42$ T ($\ell_x=20a$, $\ell_y=34a$; (black line) for $\alpha_D=14$ and $\mu=0.3t$. The vertical line shows the corresponding Zeeman shift $h=\frac{1}{2}g\mu_B B$. The inset shows the spin-polarized qp Fermi surfaces which come from the lowest (gray; red online) and the next to lowest (black) magnetic bands.

used to label the elementary excitations. We note that

$$[(i\sigma_y)\hat{\mathcal{H}}_{0,NZ}(-i\sigma_y)]^* = \sigma_y\hat{\mathcal{H}}^*_{0,NZ}\sigma_y$$
$$= -\sigma_z(\hat{\mathcal{E}}_{\mathbf{r}}-\mu)-\sigma_x\hat{\Delta}_{\mathbf{r}}$$
$$= -\hat{\mathcal{H}}_{0,NZ}. \tag{11}$$

This shows that, if we multiply an eigenvector of $\hat{\mathcal{H}}_{0,NZ}$ by $i\sigma_y$ and then take the complex conjugate of the result, then we obtain another eigenvector of the same matrix, but with the negative of the eigenvalue of the original vector. We have thus shown that the spinor $i\sigma_y\psi_{\mathbf{k}n}(\mathbf{r})$ is an eigenvector of $\hat{\mathcal{H}}_{0,NZ}$ with eigenvalue $-E_{\mathbf{k}n}$, and therefore also an eigenvector of $\hat{\mathcal{H}}_0$ with eigenvalue $-E_{\mathbf{k}n}-h$.

The fact that we can generate the negative-energy states from the positive-energy ones implies that we may take the sum in Eq. (10) to be over states that give positive eigenvalues of $\hat{\mathcal{H}}_{0,NZ}$. We could also choose, for example, the states with negative eigenvalues. In fact, we may choose any one of these two possibilities for each term. In this paper, we conform to widely used convention and use the positive energy eigenvalues.

The diagonalized Hamiltonian takes on the form

$$\hat{H}=\sum_{\mathbf{k}n}(E_{\mathbf{k}n\uparrow}\hat{\gamma}^\dagger_{\mathbf{k}n\uparrow}\hat{\gamma}_{\mathbf{k}n\uparrow}+E_{\mathbf{k}n\downarrow}\hat{\gamma}^\dagger_{\mathbf{k}n\downarrow}\hat{\gamma}_{\mathbf{k}n\downarrow})-E^{(0)}, \tag{12}$$

where $E^{(0)}=N\mu+\Sigma_{\mathbf{k}n}E_{\mathbf{k}n}$ and the qp eigenenergies are $E_{\mathbf{k}n\sigma}=E_{\mathbf{k}n}-\sigma h$. The density of states (without Zeeman) $N(\omega)=\Sigma_{n=1}^{\ell_x\ell_y}\int\frac{d^2\mathbf{k}}{\Omega_{BZ}}\delta(\omega-E_{\mathbf{k}n})$ for realistic values of the physical parameters is plotted in Fig. 2. As shown below, these energies and wave functions enter into the calculation of the NMR line shape and $1/T_1$.

In our calculations, we worked with both 20×34 and 26×26 unit cells, both of which correspond roughly to an applied field of 42 T, as well as with a 36×62 unit cell, which corresponds to an applied field of about 13 T. These calculations were done for optimally doped YBCO, for which $t=153$ meV, $\Delta_0=\frac{1}{14}t$, and $\mu=0.297t$. Because we wish to calculate thermodynamic properties of the system at low temperatures (temperatures up to 30 K), we only needed to find some of the lower energy bands. Thus, we used the Arnoldi method to find the energies and wave functions, and we discretized the reciprocal lattice into a 50×50 grid.

Let us now make some comments on the energy spectrum and the wave functions. First, we note that, while the energies $E_{\mathbf{k}n}$ are all positive, so that no quasiparticles would be present in the ground state of our system if there is no magnetic field, it is possible, under certain circumstances, for some of the energies $E_{\mathbf{k}n\uparrow}$ to be negative. To be exact, $E_{\mathbf{k}n}$ for most values of the chemical potential could exhibit a gap. If $E_{\mathbf{k}n}$ is smaller than the Zeeman splitting, then some of the energies will become negative.[20] This means that, in the ground state, there will be some quasiparticles present, all with their magnetic moments parallel to the field. This means that the "gas" of quasiparticles is spin-polarized in the ground state, resulting in a nonzero Knight shift, even at zero temperature.

B. Knight Shift and Line Shape Broadening

To find the Knight shift for a superconductor in a magnetic field, we simply substitute the Bogoliubov transformation (10) into the spin operator. Here, we only consider the effect of the spin component along the z axis,

$$\hat{S}_z(\mathbf{r})=\hat{c}^\dagger_\uparrow(\mathbf{r})\hat{c}_\uparrow(\mathbf{r})-\hat{c}^\dagger_\downarrow(\mathbf{r})\hat{c}_\downarrow(\mathbf{r}).$$

Upon performing the Bogoliubov transformation and taking the thermal average, we find that the effective magnetic field shift is

$$\delta\mathbf{B}_{eff}(\mathbf{r})=\gamma_e\hbar\sum_{\mathbf{r}'}\sum_{\mathbf{k}n}A(\mathbf{r}-\mathbf{r}')n_{\mathbf{k}n}(\mathbf{r}')[f(E_{\mathbf{k}n\downarrow})-f(E_{\mathbf{k}n\uparrow})], \tag{13}$$

where $f(E)$ is the usual Fermi-Dirac distribution,

$$f(E)=\frac{1}{e^{E/k_BT}+1}, \tag{14}$$

and $n_{\mathbf{k}n}(\mathbf{r})=|u_{\mathbf{k}n}(\mathbf{r})|^2+|v_{\mathbf{k}n}(\mathbf{r})|^2$.

Note that, even in the extreme type-II limit (i.e., taking the penetration depth to infinity), in the vortex state the local electron density is different at different locations within a magnetic unit cell. Taking into account the Zeeman shift, this translates to spatially varying spin density and by the above two equations to the spatially varying Knight shift. This means that even nuclei of the same species will have different resonance frequencies depending on their location in the magnetic unit cell. This results in a broadening of the NMR line shape (Figs. 3 and 4).

We found the effective magnetic field due to the electrons, which is proportional to the Knight shift, for the 20×34 and 36×62 lattices, and we have plotted the spatial profiles for this case in Figs. 3 and 4. As expected, the largest Knight shifts occur near the vortices because the local electron density is largest in the same area. In reality, the plots shown are for those O atoms on bonds parallel to the "short" axis of the magnetic unit cell (in this case, the x axis); the plots for the atoms on bonds along the y axis are similar in appearance.

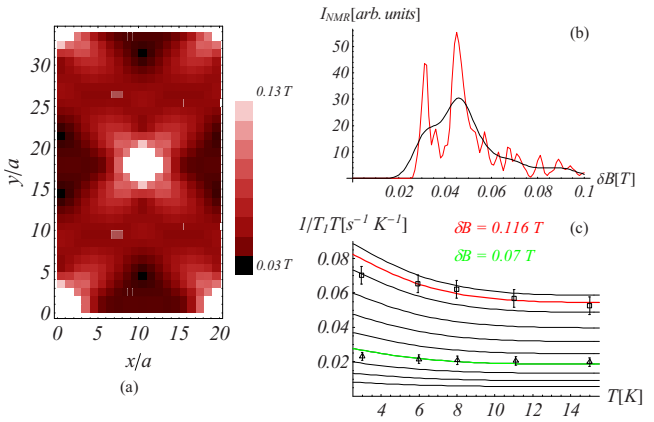

FIG. 3. (Color online) (a) Effective magnetic field shift δB_{eff} at $T=0$ as seen by the ^{17}O nuclear spins for (approximately) triangular vortex lattice corresponding to the external field $B=42$ T. The Dirac anisotropy $\alpha_D=t/\Delta_0=14$ and $\mu=0.3t$ corresponding to $x\approx 15\%$. (b) Spatial variation of δB_{eff}, whose density is shown in gray (red), leads to broadening of the NMR line shape (black) [additionally broadened by a Gaussian with $\sigma=50$ gauss (Ref. 14)]. (c) Spin-lattice relaxation rate $1/(T_1T)$ vs T for different δB_{eff}. The data points and error bars are the experimental data (Ref. 5).

We now determine the line shape that would result from this effective magnetic field. Denoting this line shape by $f(B_0)$, the line shape is given by

$$f(B_0) = \int \delta[B_0 - B(\mathbf{r})]d^3\mathbf{r}. \tag{15}$$

This formula assumes that the response of a single nucleus as a function of the frequency is a delta function centered at the resonance frequency. This, however, is not true in reality; in fact, the response has a finite width in the frequency. For this reason, we must convolute this line shape with a broadening function representing the response of a single nucleus to obtain the true line shape. The broadening function we use in our calculations is a Gaussian of width 50 G. This broadening is experimentally motivated; the width is approximately that of the $-1/2\leftrightarrow -3/2$ transition found by Mitrović.[14] Again, we calculate this line shape for 20×34 and 36×62 lattices; the results are plotted in Figs. 3 and 4.

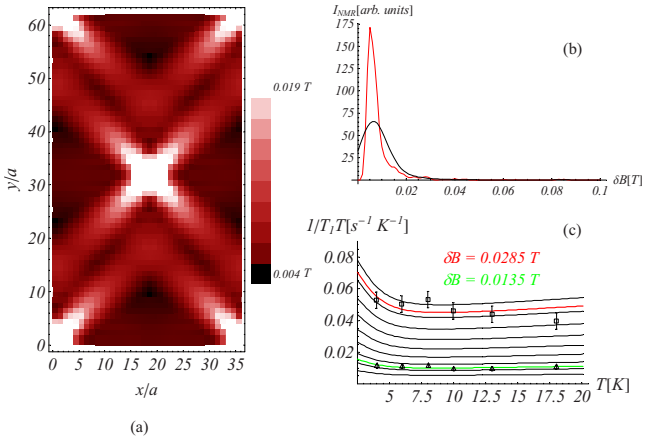

FIG. 4. (Color online) (a) Effective magnetic field shift δB_{eff} at $T=0$ as seen by the ^{17}O nuclear spins for (approximately) triangular vortex lattice corresponding to the external field $B=13$ T. All other parameters are the same as before. (b) Spatial variation of δB_{eff}, whose density is shown in gray (red), leads to broadening of the NMR line shape (black) [additionally broadened by a Gaussian with $\sigma=50$ gauss (Ref. 14)]. (c) Spin-lattice relaxation rate $1/(T_1T)$ vs T for different δB_{eff}. Again, the data points and error bars are the experimental data (Ref. 5).

C. Nuclear Spin-Lattice Relaxation Rate

To find the nuclear spin-lattice relaxation rate, $1/T_1$, we first make a simplification to the hyperfine interaction (8). Using the identity, $\hat{I}_+\hat{S}_- + \hat{I}_-\hat{S}_+ = 2(\hat{I}_x\hat{S}_x + \hat{I}_y\hat{S}_y)$, we may write it as

$$\hat{V}(\mathbf{r}) = -\gamma_e\gamma_n\hbar^2\sum_{\mathbf{R}} C(\mathbf{r}-\mathbf{R})[\hat{I}_+(\mathbf{r})\hat{S}_-(\mathbf{R}) + \hat{I}_-(\mathbf{r})\hat{S}_+(\mathbf{R})], \tag{16}$$

where, for convenience, we have defined $C=\frac{1}{2}A$. Note that we dropped the $\hat{I}_z\hat{S}_z$ term; this term will only contribute when $m=n$, and these transition rates, as we will see, do not contribute to the relaxation rate. This form will be more convenient to work with because the $\hat{S}_\pm$ operators take on simple forms, namely $\hat{S}_+=\hat{c}^\dagger_\uparrow\hat{c}_\downarrow$ and $\hat{S}_-=\hat{c}^\dagger_\downarrow\hat{c}_\uparrow$.

We now make an approximation. We assume that the nuclear Zeeman energy is much smaller than the electronic Zeeman energy, and thus we neglect that contribution to the total energy of the system. This is a good approximation if $E_m - E_n \ll k_BT$. We then obtain

$$W_{mn}(\mathbf{r}) = \frac{2\pi}{\hbar}\left\langle \sum_{QQ'} |\langle mQ'|\hat{V}(\mathbf{r})|nQ\rangle|^2\delta(E_{Q'}-E_Q)\right\rangle. \tag{17}$$

Upon expanding out the expression, $|\langle mQ'|\hat{V}(\mathbf{r})|nQ\rangle|^2$, occurring in Eq. (7), we obtain four terms; only two of these will be nonzero, namely the term involving $\langle m|\hat{I}_+|n\rangle\langle n|\hat{I}_-|m\rangle$ and the term of the same form, but with m and n interchanged. Substituting this into Eq. (7), we get

$$W_{mn}(\mathbf{r}) = \frac{2\pi}{\hbar}\gamma_e^2\gamma_n^2\hbar^4\left\langle \sum_{QQ'}\sum_{\mathbf{RR}'} C(\mathbf{r}-\mathbf{R})C(\mathbf{r}-\mathbf{R}')(\langle m|\hat{I}_+(\mathbf{r})|n\rangle \times\langle n|\hat{I}_-(\mathbf{r})|m\rangle\langle Q'|\hat{S}_-(\mathbf{R})|Q\rangle\langle Q|\hat{S}_+(\mathbf{R}')|Q'\rangle + (m\leftrightarrow n, Q'\leftrightarrow Q))\delta(E_{Q'}-E_Q)\right\rangle. \tag{18}$$

At this point, we express the spin raising and lowering operators in terms of the quasiparticle operators using the above definitions and Eq. (10), and then introduce these operators into the above expression. Upon doing so, we obtain 16 terms. However, ten of these will be zero because they will involve expressions such as $\langle Q'|\hat{\gamma}\hat{\gamma}|Q\rangle\langle Q|\hat{\gamma}\hat{\gamma}^\dagger|Q\rangle$, and it is impossible to "match" the operators in the first factor to those in the second—that is, we cannot pair, for example, an

annihilation operator in the first factor with its corresponding creation operator in the second. Of the six terms that remain, one of them, which has the form $\langle Q'|\hat{\gamma}_\downarrow\hat{\gamma}_\downarrow|Q\rangle\langle Q|\hat{\gamma}_\downarrow^\dagger\hat{\gamma}_\downarrow^\dagger|Q'\rangle$, will also be zero because the process of creating or destroying two spin-down quasiparticles violates conservation of energy due to all spin-down quasiparticles having positive energy. We note, however, that the corresponding process for spin-up quasiparticles, $\langle Q'|\hat{\gamma}_\uparrow\hat{\gamma}_\uparrow|Q\rangle\langle Q|\hat{\gamma}_\uparrow^\dagger\hat{\gamma}_\uparrow^\dagger|Q'\rangle$, does *not* violate conservation of energy because some of the spin-up quasiparticles have negative energies. This means that, in addition to the usual spin-flip (SF) scattering process, there is also a quasiparticle creation/annihilation process (PCA) through which the nuclear spins can relax.

We go into detail on how we find the different terms occurring in our final result in the Appendix; we only quote the final result here. Performing the appropriate sums and thermal averages we eventually obtain

$$W_{mn}(\mathbf{r}) = 2\pi\gamma_e^2\gamma_n^2\hbar^3[I_+^{mn}(\mathbf{r})I_-^{nm}(\mathbf{r}) + \text{c.c.}]f(\mathbf{r},T),$$

where $I_+^{mn}(\mathbf{r})=\langle m|I_+(\mathbf{r})|n\rangle$, and similarly for $I_-^{mn}(\mathbf{r})$. This in turn gives the main result of this paper,

$$\frac{1}{T_1(\mathbf{r})} = 4\pi\gamma_e^2\gamma_n^2\hbar^3 f(\mathbf{r},T), \tag{19}$$

where the function

$$f(\mathbf{r},T) = \sum_{nn'}\int\frac{d^2\mathbf{k}}{\Omega_{BZ}}\frac{d^2\mathbf{k}'}{\Omega_{BZ}}\left[\frac{|G^{\text{SF}}_{\mathbf{k}n\mathbf{k}'n'}(\mathbf{r})|^2\delta(E_{\mathbf{k}n}-E_{\mathbf{k}'n'}+2h)}{4\cosh^2\left(\frac{E_{\mathbf{k}n}+h}{2k_BT}\right)} + \frac{|G^{\text{PCA}}_{\mathbf{k}n\mathbf{k}'n'}(\mathbf{r})|^2\delta(E_{\mathbf{k}n}+E_{\mathbf{k}'n'}-2h)}{8\cosh^2\left(\frac{E_{\mathbf{k}n}-h}{2k_BT}\right)}\right]. \tag{20}$$

The above integrals are over the 1st Brillouin zone whose area is $\Omega_{BZ}=4\pi^2/(\ell_x\ell_y)$. The qp coherence factors enter via the functions

$$G^{\text{SF}}_{\mathbf{k}n\mathbf{k}'n'}(\mathbf{r}) = \sum_{\mathbf{R}} C_{\mathbf{r}-\mathbf{R}}[U^*_{\mathbf{k}n}(\mathbf{R})U_{\mathbf{k}'n'}(\mathbf{R}) + V^*_{\mathbf{k}n}(\mathbf{R})V_{\mathbf{k}'n'}(\mathbf{R})]e^{i(\mathbf{k}'-\mathbf{k})\cdot\mathbf{R}}$$

and

$$G^{\text{PCA}}_{\mathbf{k}n\mathbf{k}'n'}(\mathbf{r}) = \sum_{\mathbf{R}} C_{\mathbf{r}-\mathbf{R}}[V_{\mathbf{k}n}(\mathbf{R})U_{\mathbf{k}'n'}(\mathbf{R}) - U_{\mathbf{k}n}(\mathbf{R})V_{\mathbf{k}'n'}(\mathbf{R})]e^{i(\mathbf{k}'+\mathbf{k})\cdot\mathbf{R}}.$$

Note that this differs from the formulas presented in Refs. 10 and 13, most importantly by the presence of the second term. The eigenenergies $E_{n\mathbf{k}}\geq 0$ are the solutions of the Bogoliubov-de Gennes equation without the Zeeman coupling, and the corresponding periodic wave functions are normalized within the magnetic unit cell: $\Sigma_{\mathbf{r}\in\ell_x\ell_y}(|U_{\mathbf{k}n}|^2(\mathbf{r})+|V_{\mathbf{k}n}|^2(\mathbf{r}))=1$. From Eqs. (19) and (20) it is readily seen that, regardless of the minimal value of $E_{n\mathbf{k}}$, at temperatures $T\ll h=\frac{1}{2}g\mu_BB$, the qp SF process is activated and thus vanishingly small. At $B=42$ T this corresponds to a temperature scale of $\sim$28 K, which in turn means that the low $T(\sim 5$ K) upturn in $1/(T_1T)$ observed experimentally[3,5] cannot be due to this process. It is the second term (PCA) which dominates at low temperatures and corresponds to the observed effect.

To illustrate the basic physics behind the effect, we will temporarily ignore the orbital effects and analyze the consequences of the Zeeman coupling alone.[23] Physically, this would correspond to a thin film in a parallel (in-plane) B field. The eigenenergies in Eq. (20) are then easily found to be $E_{\mathbf{k}}=\sqrt{\epsilon_{\mathbf{k}}^2+\Delta_{\mathbf{k}}^2}$, where $\epsilon_{\mathbf{k}}=-2t(\cos k_xa+\cos k_ya)-\mu$ and $\Delta_{\mathbf{k}}=2\Delta_0(\cos k_xa-\cos k_ya)$. At the same time the wave functions are simply $u_{\mathbf{k}}=\frac{1}{\sqrt{2}}\sqrt{1+\frac{\epsilon_{\mathbf{k}}}{E_{\mathbf{k}}}}$ and $v_{\mathbf{k}}=\frac{\text{sgn}\,\Delta_{\mathbf{k}}}{\sqrt{2}}\sqrt{1-\frac{\epsilon_{\mathbf{k}}}{E_{\mathbf{k}}}}$. Assuming for simplicity $C_{\mathbf{r}}=c_0\delta_{\mathbf{r},0}$ and particle-hole symmetry, this gives for the Zeeman-only case

$$\frac{1}{T_1} = 2\pi\gamma_e^2\gamma_n^2\hbar^3c_0^2 \times\left(\int_0^\infty dE\frac{N(E)N(E+2h)}{4\cosh^2\left(\frac{E+h}{2T}\right)} + \int_0^{2h}dE\frac{N(E)N(2h-E)}{8\cosh^2\left(\frac{E-h}{2T}\right)}\right). \tag{21}$$

For h, $T\ll\Delta_0$ we need only the low-energy qp density of states, which is $N(E)=2E/(\pi v_Fv_\Delta)$, where $v_F=2\sqrt{2}at\sqrt{1-\frac{\mu^2}{16t^2}}$ and $v_\Delta=v_F\Delta_0/t$. In this limiting case, the integral can be found in a closed form and

$$\frac{1}{T_1} = \frac{4}{\pi}\frac{\gamma_e^2\gamma_n^2\hbar^3c_0^2}{v_F^2v_\Delta^2}T^3F\left(\frac{h}{T}\right), \tag{22}$$

where $F(x)=\pi^2+8x\ln(1+e^x)-3x^2+8Li_2(-e^x)$ and $Li_s(z)$ is the polylogarithm. For $x\ll 1$, $F(x)=\frac{\pi^2}{3}-x^2$, and in this limit we recover the standard d wave $1/(T_1T)\sim T^2$. On the other hand, for $x\gg 1$, $F(x)=x^2-\frac{\pi^2}{3}$. In this limit $1/(T_1T)$ increases as T is lowered and approaches a constant at $T=0$. The minimum in $1/(T_1T)$ then results from the competition between the spin-flip process, which dominates at $T\gg h$ and the qp pair creation/annihilation process which dominates at $T\ll h$.

Putting back the coupling of the B field to the orbital motion of the electrons, we find that the effect described above acquires an interesting spatial content. The dispersing states which are pulled below zero energy by the Zeeman coupling are strongly concentrated around the cores. Due to the increase of the low-energy wave functions near the cores, the low-temperature relaxation rate of the nuclear spin is the largest in the vicinity of the cores and *decreases* with increasing T. This temperature dependence is in turn due to the pair creation/annihilation processes, i.e., the second term in Eq. (20).

To generate a dependence of the spin-lattice relaxation rate on the internal magnetic field, we associated the rate at a given point and a given temperature with the value of the effective magnetic field shift at that point and temperature. We then fit this set of points to a power law to generate a continuous dependence; at all magnetic field shifts of interest, the points are close enough together that they approximately form a continuum. We do this for all temperatures up

to 30 K for $B=42$ T and up to 20 K for $B=13$ T; the results of this procedure are shown in Figs. 3 and 4. We also highlight the curves that give the best fit to the data near the vortex core and away from the core.[3,5]

IV. CONTRIBUTION OF ANTIFERROMAGNETC CORRELATIONS TO THE SPIN-LATTICE RELAXATION RATE

We now address the issue of how much of an effect antiferromagnetic correlations will have on the spin-lattice relaxation rate of ^{17}O in the vortex state, assuming that the vortex cores represent normal-state regions. As was mentioned before, it is known that the form factor filters out such correlations in the normal state.[18] Within the simple model presented here, we find that this filtering is still active in the vortex state. To investigate the effect of vortices, we used a modification of the phenomenological model set forth, among others, by Zha, Barzykin, and Pines.[18] We start with their expression for the "antiferromagnetic" part of the susceptibility,

$$\chi_{\mathrm{AF}}(\mathbf{k},\omega)=\frac{1}{4}\sum_{i}\frac{\alpha\xi^2\mu_B}{1+(\mathbf{q}-\mathbf{Q}_i)^2+i\omega/\omega_{\mathrm{SC}}}. \tag{23}$$

Here, α is a scale factor, ξ is the antiferromagnetic correlation length, μ_B is the Bohr magneton, the $\mathbf{Q}_i$ are the locations of the peaks in the susceptibility found from neutron scattering experiments, ω_{SC} is the characteristic frequency of spin fluctuations, and $\mathbf{q}$ ranges over the entire first Brillouin zone.[18] We obtained the model we used by rewriting the above susceptibility as a function of position, separating the position dependence into a dependence on the position of a "magnetic unit cell" and a dependence on position within the cell, and Fourier transforming the result with respect to the magnetic unit cell position. The result is

$$\chi_{\mathrm{AF}}(\mathbf{q},\delta\mathbf{r}-\delta\mathbf{r}',\omega)=\frac{1}{4}\frac{N_M}{N}\sum_{\mathbf{G}}\sum_{i}\frac{\alpha\xi^2\mu_B e^{i(\mathbf{q}+\mathbf{G})\cdot(\delta\mathbf{r}-\delta\mathbf{r}')}}{1+(\mathbf{q}+\mathbf{G}-\mathbf{Q}_i)^2+i\omega/\omega_{\mathrm{SC}}}, \tag{24}$$

where $\mathbf{q}$ now ranges over the first magnetic Brillouin zone, $\mathbf{G}$ is the set of all vectors such that $e^{i\mathbf{G}\cdot\mathbf{R}}=1$ for all $\mathbf{R}$ in the magnetic lattice and such that $\mathbf{q}+\mathbf{G}$ is within the first atomic Brillouin zone, N_M is the number of magnetic unit cells, and N is the number of sites in the atomic lattice. We note that, assuming an $L_x\times L_y$ magnetic unit cell, the number of atomic sites is just $L_xL_yN_M$, so we may simply write

$$\chi_{\mathrm{AF}}(\mathbf{q},\delta\mathbf{r}-\delta\mathbf{r}',\omega)=\frac{1}{4}\frac{1}{L_xL_y}\sum_{\mathbf{G}}\sum_{i}\times\frac{\alpha\xi^2\mu_B e^{i(\mathbf{q}+\mathbf{G})\cdot(\delta\mathbf{r}-\delta\mathbf{r}')}}{1+(\mathbf{q}+\mathbf{G}-\mathbf{Q}_i)^2+i\omega/\omega_{\mathrm{SC}}}. \tag{25}$$

So far, we have not introduced a new model; we only rewrote the original in a more complicated form. We will now modify this model to introduce vortex effects. For simplicity, we will assume only one vortex per unit cell. We model these effects by simply introducing step functions into the susceptibility to restrict the antiferromagnetic correlations to within a distance equal to the superconducting coherence length ξ_{SC} from the center of the vortex. The result is

$$\chi_{\mathrm{AF}}(\mathbf{q},\delta\mathbf{r},\delta\mathbf{r}',\omega)=\frac{1}{4}\frac{1}{L_xL_y}\sum_{\mathbf{G}}\sum_{i}\frac{\alpha\xi^2\mu_B e^{i(\mathbf{q}+\mathbf{G})\cdot(\delta\mathbf{r}-\delta\mathbf{r}')}}{1+(\mathbf{q}+\mathbf{G}-\mathbf{Q}_i)^2+i\omega/\omega_{\mathrm{SC}}}\times\theta(\xi_{\mathrm{SC}}-\delta r)\theta(\xi_{\mathrm{SC}}-\delta r'). \tag{26}$$

We now turn our attention to finding the spin-lattice relaxation rate from this susceptibility. It can be shown that, if we assume that this relaxation is due to the hyperfine interaction (8), then the spin-lattice relaxation rate will be

$$\frac{1}{T_1(\mathbf{r})}=\gamma_e^2\gamma_n^2\hbar^3k_BT\sum_{\mathbf{r}'\mathbf{r}''}A(\mathbf{r}-\mathbf{r}')A(\mathbf{r}-\mathbf{r}'')\times\lim_{\omega\to0}\frac{\mathrm{Di}\,\chi_{+-}(\mathbf{r}',\mathbf{r}'',\omega)}{\hbar\omega}, \tag{27}$$

where $\mathrm{Di}\,f(\ldots,\omega)$ is a "discontinuity" operator, defined as

$$\mathrm{Di}\,f(\ldots,\omega)=\frac{f(\ldots,\omega+i0^+)-f(\ldots,\omega-i0^-)}{2i}. \tag{28}$$

We may rewrite the above formula for a susceptibility of the form we are working with. By introducing the appropriate Fourier transforms, we eventually arrive at the desired result,

$$\frac{1}{T_1(\mathbf{r})}=\gamma_e^2\gamma_n^2\hbar^3k_BT\frac{1}{L_x^2L_y^2N_M}\times\sum_{\delta\mathbf{r}'\,\delta\mathbf{r}''}\sum_{\mathbf{G}_1\mathbf{G}_2}\sum_{\mathbf{k}}A(\mathbf{k}+\mathbf{G}_1)A^*(\mathbf{k}+\mathbf{G}_2)e^{i(\mathbf{G}_1-\mathbf{G}_2)\cdot\mathbf{r}}\times e^{-i(\mathbf{k}+\mathbf{G}_1)\cdot\delta\mathbf{r}'}e^{i(\mathbf{k}+\mathbf{G}_2)\cdot\delta\mathbf{r}''}\lim_{\omega\to0}\frac{\mathrm{Di}\,\chi_{+-}(\mathbf{k},\delta\mathbf{r}',\delta\mathbf{r}'',\omega)}{\hbar\omega}, \tag{29}$$

where $\delta\mathbf{r}'$ and $\delta\mathbf{r}''$ are summed over the entire unit cell, $\mathbf{k}$ is summed over the entire magnetic Brillouin zone, and $\mathbf{G}_1$ and $\mathbf{G}_2$ are summed over the same set of vectors as $\mathbf{G}$ in Eq. (25).

The rest of our work was done numerically. We used the experimentally-determined parameters given by Barzykin and Pines for the susceptibility for $YBa_2Cu_3O_{6.63}$.[24] We first performed a numerical calculation of the rates for $\mathbf{r}=0$ for both copper and oxygen without vortices. The form factors we used are

$$A_{\mathrm{Cu}}(\mathbf{k})=A+2B(\cos k_xa+\cos k_ya), \tag{30}$$

$$A_{\mathrm{O},x}(\mathbf{k})=2\cos\frac{1}{2}k_xa(C_1+2C_2\cos k_ya), \tag{31}$$

$$A_{\mathrm{O},y}(\mathbf{k})=2\cos\frac{1}{2}k_ya(C_1+2C_2\cos k_xa), \tag{32}$$

where a is the atomic lattice spacing and the parameters, A, B, C_1, and C_2 are those given by Zha, Barzykin, and Pines.[18] Because of the fact that the momentum-space points (k_x,k_y)

and (k_y,k_x) are both present in the sums in our formulas, Eqs. (31) and (32) should give the same result. We did this using both Eqs. (23) and (25) to check our formulas. The temperature range we examined was $70\ \mathrm{K} \leq T \leq 300\ \mathrm{K}$. We found that the contributions to the rates for both Cu and O decreased with increasing temperature, and that the rates for O were several orders of magnitude smaller than for Cu; such suppression of the rate for O compared to Cu has been reported before by Mila and Rice.[16] We then repeated this calculation, this time including vortices. We set the superconducting coherence length $\xi_{SC}=2a$. We found that the temperature dependence of both rates was qualitatively the same as before, but that the rates were actually enhanced; the copper rates by an entire order of magnitude and the oxygen rates by a factor of about 4. We believe that this is due to the fact that, by imposing the distance cutoff, we removed contributions to the relaxation rate that would have reduced the rate. Based on this simplified model, we therefore expect that, not only is the filtering effect still present in the mixed state, but it is, in fact, enhanced.

It goes without saying then that this filtering effect would therefore make oxygen NMR more sensitive to the PCA processes than copper NMR. This is because the effect of antiferromagnetic correlations is much less for oxygen than for copper, meaning that the PCA processes will dominate in oxygen.

V. CONCLUSIONS

In this work, we argued that it is possible to explain the broadening of the line shape and the upturn in the spin-lattice relaxation rate with decreasing temperature observed experimentally[3,5] without introducing antiferromagnetic correlations. The line shape broadening can be explained, at least in part, by noting that the Knight shift varies with position in the lattice in the vortex state. This position dependence leads to each nucleus having a different resonance frequency, and therefore to a broadened line shape. The upturn in the relaxation rate can be explained as due to a second relaxation process, namely creation and annihilation of pairs of spin-up quasiparticles, that appears when a magnetic field is applied, and this process dominates at low temperatures. We do not wish to claim that AF correlations do not exist in YBCO, only that certain features of the NMR data once attributed to such correlations can be explained without them; in fact, there is other evidence for the existence of such correlations, namely neutron scattering data.[25] As we argued in Sec. IV, even in the presence of AF correlations, the spin-lattice relaxation rates for O will not be greatly affected by them due to the form factor.

Based on the above arguments we expect that, once the vortex lattice melts and the system enters a vortex liquid phase, the NMR lines sharpen due to motional narrowing.[26,27] At the same time, we expect that the spin-lattice relaxation rate, $1/T_1$, is determined by the faster rates and that the low T upturn persists in the vortex liquid.

This picture and the density of states shown in Fig. 2 also predict that if an experiment is performed in a clean thin film with a well-ordered vortex lattice in which the perpendicular component of the B field is kept fixed, while changing the magnitude of the total **B**, *quantumlike oscillations* in $1/T_1$, due to the oscillations of the density of states *in energy*, would be observed.

While our calculated line shapes have about the same width as the experimental shape for the 42 T case, the shapes for the 13 T case have different widths. One possible contributing factor to this discrepancy is the fact that we neglected the variation of the magnetic field and the pairing amplitude over a unit cell. We expect the magnetic field to vary more strongly in the 13 T case than in the 42 T case because the vortices are further apart in the 13 T case. In fact, in the 42 T case, the distance between the two vortices in a unit cell is about 10% of the penetration depth, while, in the 13 T case, this distance is about 23% of the penetration depth. This variation will introduce further broadening, which will be greater at 13 T than at 42 T, consistent with our findings.

We also notice that the "tails" on our calculated curves are different in length than those of the experimental curves. We believe that this, once again, is due to the fact that we neglected the variation of the pairing potential over a unit cell. In reality, the order parameter should be lower in magnitude near the vortex cores because these regions are where superconductivity is beginning to break down. This means that we expect our calculated line shapes to be more accurate in the lower internal field regions than in the high internal field regions.

Finally, we note that the peak in our curve at 42 T is split in two, as opposed to the single peak seen in the experimental data.[3,5] This suggests that there is another broadening mechanism at work besides that due to the finite width of the normal-state line shape because such broadening can wash out the "split" peak so that only a single peak appears. One such possibility is the presence of impurities.

We are able to obtain good fits of our calculated temperature dependence of the spin-lattice relaxation rates to the experimental data using the internal magnetic field as our *only* fitting parameter. We note, however, that the values of the internal magnetic fields giving us our best-fit curves on the line shape do not quite match the experimental results. In the experiment, the region away from the core was in the vicinity of the peak in the line shape.[5] However, the positions of the corresponding theoretical curves do not quite fall on the peak; rather, they are away from it. It is possible that this discrepancy may be due, in part, to our approximations in solving the Bogoliubov-de Gennes equation, and that more realistic modeling of the vortex core is necessary to account for this.

ACKNOWLEDGMENTS

We wish to thank Mitrović, Kivelson, Chakravarty, and Tešanović for discussion. O.V. would also like to thank the Aspen Center for Physics, where part of this work was completed, for hospitality.

APPENDIX: DETAILS OF DERIVATION OF SPIN-LATTICE RELAXATION RATE

Here, we go into some more detail about how we found the different terms in the spin-lattice relaxation rate. As we

mentioned earlier, when we rewrite the spin raising and lowering operators in terms of the Bogoliubov quasiparticles, we obtain 16 terms, though only six give nonzero contributions. One term we find that contributes to the SF process, suppressing factors of u and v that occur, is

$$\sum_{QQ'}\sum_{\mathbf{k}n\mathbf{k}'n'}\sum_{\mathbf{q}m\mathbf{q}'m'}\langle Q'|\hat{\gamma}^{\dagger}_{\mathbf{k}n\downarrow}\hat{\gamma}_{\mathbf{k}'n'\uparrow}|Q\rangle\langle Q|\hat{\gamma}^{\dagger}_{\mathbf{q}m\uparrow}\hat{\gamma}_{\mathbf{q}'m'\downarrow}|Q'\rangle \times\delta(E_{Q'}-E_Q). \tag{A1}$$

We note that the only terms that will give nonzero contributions are those for which $\mathbf{k}=\mathbf{q}'$, $\mathbf{k}'=\mathbf{q}$, $n=m'$, and $n'=m$. We may then write

$$\sum_{QQ'}\sum_{\mathbf{k}n\mathbf{k}'n'}\langle Q'|\hat{\gamma}^{\dagger}_{\mathbf{k}n\downarrow}\hat{\gamma}_{\mathbf{k}'n'\uparrow}|Q\rangle\langle Q|\hat{\gamma}^{\dagger}_{\mathbf{k}'n'\uparrow}\hat{\gamma}_{\mathbf{k}n\downarrow}|Q'\rangle \times\delta(E_{Q'}-E_Q). \tag{A2}$$

We now note that the only nonzero matrix elements will be those in which the state Q' is obtained from the state Q by scattering a particle from the state with crystal wave vector $\mathbf{k}'$, band index n', and spin up into the state with wave vector $\mathbf{k}$, band index n, and spin down. This means that the energy difference between the two states is just $E_{Q'}-E_Q=E_{\mathbf{k}n\downarrow}-E_{\mathbf{k}'n'\uparrow}=E_{\mathbf{k}n}-E_{\mathbf{k}'n'}+2h$. This energy difference is independent of the exact many-particle states Q and Q', so we may rewrite the sum on these states as a trace,

$$\sum_{Q'}\sum_{\mathbf{k}n\mathbf{k}'n'}\langle Q'|\hat{\gamma}^{\dagger}_{\mathbf{k}n\downarrow}\hat{\gamma}_{\mathbf{k}'n'\uparrow}\hat{\gamma}^{\dagger}_{\mathbf{k}'n'\uparrow}\hat{\gamma}_{\mathbf{k}n\downarrow}|Q'\rangle\delta(E_{\mathbf{k}n}-E_{\mathbf{k}'n'}+2h). \tag{A3}$$

We may now employ the anticommutation relations among the quasiparticle operators to rewrite the above in terms of number operators

$$\sum_{Q'}\sum_{\mathbf{k}n\mathbf{k}'n'}\langle Q'|\hat{n}_{\mathbf{k}n\downarrow}(1-\hat{n}_{\mathbf{k}'n'\uparrow})|Q'\rangle\delta(E_{\mathbf{k}n}-E_{\mathbf{k}'n'}+2h). \tag{A4}$$

Upon taking the thermal average, the trace becomes a product of Fermi functions,

$$\sum_{\mathbf{k}n\mathbf{k}'n'}f(E_{\mathbf{k}n\downarrow})(1-f(E_{\mathbf{k}'n'\uparrow}))\delta(E_{\mathbf{k}n}-E_{\mathbf{k}'n'}+2h). \tag{A5}$$

We will also show the calculation for the term resulting from the pair creation and annihilation term because it will differ slightly from the calculation given above. This term (again suppressing actors of u and v) is

$$\sum_{QQ'}\sum_{\mathbf{k}n\mathbf{k}'n'}\sum_{\mathbf{q}m\mathbf{q}'m'}\langle Q'|\hat{\gamma}_{\mathbf{k}n\uparrow}\hat{\gamma}_{\mathbf{k}'n'\uparrow}|Q\rangle\langle Q|\hat{\gamma}^{\dagger}_{\mathbf{q}m\uparrow}\hat{\gamma}^{\dagger}_{\mathbf{q}'m'\uparrow}|Q'\rangle \times\delta(E_{Q'}-E_Q). \tag{A6}$$

In this case, there are two ways to "match" the operators; we may either let $(\mathbf{k},n)=(\mathbf{q},m)$ and $(\mathbf{k}',n')=(\mathbf{q}',m')$ or let $(\mathbf{k},n)=(\mathbf{q}',m')$ and $(\mathbf{k}',n')=(\mathbf{q},m)$. We thus obtain

$$\sum_{QQ'}\sum_{\mathbf{k}n\mathbf{k}'n'}(\langle Q'|\hat{\gamma}_{\mathbf{k}n\uparrow}\hat{\gamma}_{\mathbf{k}'n'\uparrow}|Q\rangle\langle Q|\hat{\gamma}^{\dagger}_{\mathbf{k}n\uparrow}\hat{\gamma}^{\dagger}_{\mathbf{k}'n'\uparrow}|Q'\rangle + \langle Q'|\hat{\gamma}_{\mathbf{k}n\uparrow}\hat{\gamma}_{\mathbf{k}'n'\uparrow}|Q\rangle\langle Q|\hat{\gamma}^{\dagger}_{\mathbf{k}'n'\uparrow}\hat{\gamma}^{\dagger}_{\mathbf{k}n\uparrow}|Q'\rangle)\delta(E_{Q'}-E_Q). \tag{A7}$$

The only nonzero matrix elements in this case are those in which the state Q' is obtained from the state Q by destroying two quasiparticles with spin up, one with wave vector $\mathbf{k}$ and band index n and one ith wave vector $\mathbf{k}'$ and band index n'. This means that the energy difference $E_{Q'}-E_Q=-E_{\mathbf{k}n\uparrow}-E_{\mathbf{k}'n'\uparrow}=-E_{\mathbf{k}n}-E_{\mathbf{k}'n'}+2h$. The rest of the derivation proceeds as before, and we eventually obtain

$$\sum_{\mathbf{k}n\mathbf{k}'n'}[1-f(E_{\mathbf{k}n\uparrow})](1-f(E_{\mathbf{k}'n'\uparrow}))\delta(E_{\mathbf{k}n}+E_{\mathbf{k}'n'}-2h). \tag{A8}$$

[1] R. E. Walstedt, *The NMR Probe of High-Tc Materials by Walstedt* (Springer-Verlag, Berlin, 2008).

[2] N. J. Curro, C. Milling, J. Haase, and C. P. Slichter, Phys. Rev. B **62**, 3473 (2000).

[3] V. F. Mitrović, E. E. Sigmund, M. Eschrig, H. N. Bachman, W. P. Halperin, A. P. Reyes, P. Kuhns, and W. G. Moulton, Nature (London) **413**, 501 (2001).

[4] K. Kakuyanagi, K. Kumagai, and Y. Matsuda, Phys. Rev. B **65**, 060503(R) (2002).

[5] V. F. Mitrović, E. E. Sigmund, W. P. Halperin, A. P. Reyes, P. Kuhns, and W. G. Moulton, Phys. Rev. B **67**, 220503(R) (2003).

[6] S. A. Kivelson, I. P. Bindloss, E. Fradkin, V. Organesyan, J. M. Tranquada, A. Kapitulnik, and C. Howald, Rev. Mod. Phys. **75**, 1201 (2003).

[7] P. A. Lee, N. Nagaosa, and X.-G. Wen, Rev. Mod. Phys. **78**, 17 (2006).

[8] M. Takigawa, A. P. Reyes, P. C. Hammel, J. D. Thompson, R. H. Heffner, Z. Fisk, and K. C. Ott, Phys. Rev. B **43**, 247 (1991).

[9] C. P. Slichter, *Principles of Magnetic Resonance*, 3rd ed. (Springer, New York, 1996), p. 151.

[10] M. Takigawa, M. Ichioka, and K. Machida, Phys. Rev. Lett. **83**, 3057 (1999).

[11] Y. Wang and A. H. MacDonald, Phys. Rev. B **52**, R3876 (1995).

[12] R. Wortis, A. J. Berlinsky, and C. Kallin, Phys. Rev. B **61**, 12342 (2000).

[13] D. Knapp, C. Kallin, A. J. Berlinsky, and R. Wortis, Phys. Rev. B **66**, 144508 (2002).

[14] V. F. Mitrović, Ph. D. thesis, Northwestern University, 2001.

[15] B. S. Shastry, Phys. Rev. Lett. **63**, 1288 (1989).

[16] F. Mila and T. M. Rice, Physica C **157**, 561 (1989).

[17] A. J. Millis, H. Monien, and D. Pines, Phys. Rev. B **42**, 167 (1990).

[18] Y. Zha, V. Barzykin, and D. Pines, Phys. Rev. B **54**, 7561 (1996).
[19] O. Vafek, A. Melikyan, M. Franz, and Z. Tešanović, Phys. Rev. B **63**, 134509 (2001); O. Vafek, A. Melikyan, and Z. Tesanovic, *ibid.* **64**, 224508 (2001).
[20] O. Vafek and A. Melikyan, Phys. Rev. Lett. **96**, 167005 (2006); A. Melikyan and O. Vafek, Phys. Rev. B **78**, 020502(R) (2008).
[21] A. Melikyan and Z. Tešanović, Phys. Rev. B **74**, 144501 (2006).
[22] M. Franz and Z. Tešanović, Phys. Rev. Lett. **84**, 554 (2000).
[23] K. Yang and S. L. Sondhi, Phys. Rev. B **57**, 8566 (1998).
[24] V. Barzykin and D. Pines, Phys. Rev. B **52**, 13585 (1995).
[25] D. Vaknin, J. L. Zarestky, and L. L. Miller, Physica C **329**, 109 (2000).
[26] A. P. Reyes, X. P. Tang, H. N. Bachman, W. P. Halperin, J. A. Martindale, and P. C. Hammel, Phys. Rev. B **55**, R14737 (1997).
[27] C. Kittel, *Introduction to Solid State Physics*, 4th ed. (Wiley, New York, 1971), p. 586.